

## Pulsed Melting of Silicon (111) and (100) Surfaces Simulated by Molecular Dynamics

Farid F. Abraham

*IBM Research Laboratory, San Jose, California 95193*

and

Jeremy Q. Broughton

*Materials Science Department, State University of New York at Stony Brook, Stony Brook, New York 11794*

(Received 28 October 1985)

The pulsed heating of Si (100) and (111) surfaces has been simulated by molecular dynamics. The (111) crystal-melt interface propagates by layer-by-layer growth whereas the (100) interface grows in a continuous fashion. The equilibrium crystal-melt interface is sharp for the (111) orientation and broad for the (100) orientation. These simulations are the first use of nonpairwise potentials to study interfaces between condensed phases, and the results support models of interfaces which heretofore had to be deduced from indirect experimental information.

PACS numbers: 68.45.-v, 64.70.Dv

The purpose of statistical mechanical simulation is not only to describe materials properties at an atomistic level but also to predict behavior under conditions not experimentally accessible or not yet tried. For the simplest systems such as the inert gases and ionic materials, the state-of-the-art has probably achieved many of these objectives. This is not presently true for more complex covalent and/or metallicly bonded systems. The problem here is not only a lack of knowledge of good potential functions to describe the interaction between atoms but also the lack of computer power that such complex potentials require for their configuration-space exploration.

Silicon is a case in point. Although a harmonic potential for low-temperature crystalline Si has been known for some time,<sup>1</sup> it is only recently that potentials capable of approximately describing its high-temperature states have been developed.<sup>2-6</sup> The calculation of the force on each atom takes  $\sim 3$  times longer to evaluate than for Lennard-Jones atoms at normal densities. This paper describes an intercomparative study by molecular dynamics of the pulsed heating of the (100) and (111) surfaces using the Stillinger-Weber (SW) potential<sup>3</sup> (described below) with emphasis on the growth characteristics of the melt and the subsequently achieved equilibrium crystal-melt interface. Since this potential was optimized along an isochore for the bulk crystal and liquid phases, we expect it to describe the interface between the two phases rather accurately. Our isobaric calculations of the triple-point properties further illustrate the quality of the SW potential. The simulation results support expectations that until now have only been deduced from indirect experimental observation, the details of which we now describe.

At room temperature the (111) crystal-vapor surface stabilizes in the well-known  $7 \times 7$  structure.<sup>7</sup> A univer-

sally accepted atomistic model of this system is still lacking. At higher temperatures, a  $1 \times 1$  pattern is observed which has been interpreted by some as due to an amorphous (disordered) overlayer and by others as single termination of the bulk.<sup>8</sup> The (100) surface forms a  $2 \times 1$  structure which has been interpreted as being due to the formation of Si-Si dimers in the top layer.<sup>9,10</sup> We do not expect the SW potential to describe the  $7 \times 7$  structure properly since it is generally believed that rehybridization of surface orbitals is a cause of this reconstruction.<sup>7</sup> The SW potential favors tetrahedral bonding. On the other hand, the driving force for (100) dimer formation is thought to be caused by silicon's attempt to achieve tetrahedrality.<sup>9,10</sup> Preliminary results using the SW potential do show in-plane dimer formation.<sup>11,12</sup> In the Czochralski growth of Si from the melt it is known that a slight undercooling exists at the (111) interface but not at any of the other faces.<sup>13</sup> This implies that the (111) interface is just below its roughening transition and grows by a layerwise mechanism. The other faces are above roughening and grow without nucleation by a continuous process. The (111) interface is expected to be smooth and sharp; the (100) rough and broad.

The SW potential energy (PE) of the system is given as the sum over all pairs of atoms of a Lennard-Jones-type term of depth  $\epsilon$  which smoothly goes to zero at a distance  $a$  (approximately the second-neighbor distance) plus the sum over all triplets of a three-body term of the form

$$\phi_3(r_{ij}, r_{ik}, \theta_{jik}) = \lambda \exp[\gamma(r_{ij} - a)^{-1} + \gamma(r_{ik} - a)^{-1}] \times (\cos\theta_{jik} + \frac{1}{3})^2.$$

This term vanishes if either  $r_{ij}$  or  $r_{ik}$  is greater than  $a$ . The angular term is zero at the ideal tetrahedral angle and positive otherwise.

Each of the (111) and (100) systems were periodically connected in the  $x$ ,  $y$ , and  $z$  directions with sufficient extent in the  $z$  to allow for vapor phase. The standard techniques of molecular dynamics were applied. Properties are reported in the reduced units of the SW paper; that is, the unit of length is 0.20951 nm, the unit of energy is  $3.4723 \times 10^{-19}$  J, and the unit of mass ( $^{28}\text{Si}$ ) is  $4.6459 \times 10^{-26}$  kg. The systems each comprise approximately 1800 atoms and were equilibrated for  $20\,000 \Delta t$  ( $\Delta t = 3.8 \times 10^{-16}$  sec) at a reduced temperature of 0.070 (1760 K), our best guess for the triple point. The  $x$ - $y$  period was set by use of the density from a zero-pressure bulk-crystal calculation at this temperature. Neither the (111) nor (100) systems exhibited interface melting in contrast with the same faces of a fcc Lennard-Jones system at its triple point.<sup>14</sup> The (111) surface, in accord with the conclusion of high-temperature LEED experiments,<sup>8</sup> exhibits a structure which is simple termination of the bulk. The kinetic energy of the top four layers was then instantaneously raised on one side of the slab a sufficient amount to cause approximately half the system to eventually melt. Whereas we were able to guess the amount of energy to be added to do this for the (111) surface, our first attempt on the (100) produced only a limited amount of melt. After the latter equilibrated, further kinetic energy was added and it is the results of this experiment which are reported below. The history of the constant-energy systems was followed until equilibrium was again achieved.

After the heat pulse (time zero), it took  $\sim 60\,000 \Delta t$  for the system to reach equilibrium, that is, for the total system temperature to be invariant with time and for the temperature profile through the system to be flat. Figure 1 gives trajectory plots in a thin  $x$ - $z$  section

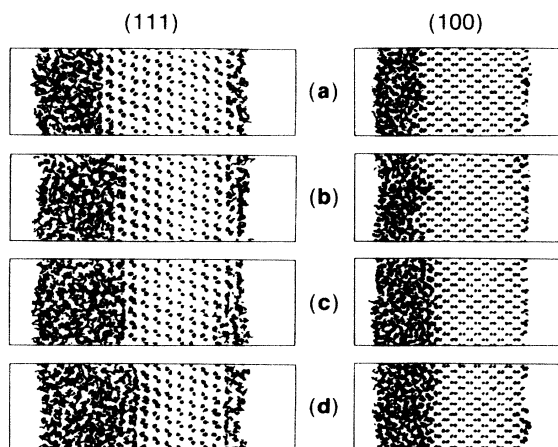


FIG. 1. Trajectory plots of thin  $x$ - $z$  slice through (111) and (100) systems covering elapsed time ranges of (a)  $(15-20) \times 10^3 \Delta t$ , (b)  $(25-30) \times 10^3 \Delta t$ , (c)  $(45-50) \times 10^3 \Delta t$ , and (d)  $(95-100) \times 10^3 \Delta t$ .

for the (111) and (100) interfaces as a function of time. The (111) melt front clearly progresses a layer at a time which we expect by microscopic reversibility from Czochralski-crystal-growth experiments. Trajectory plots in the  $x$ - $y$  plane and for other  $x$ - $z$  sections show the front to be flat in the  $x$ - $y$  plane. In contrast, the (100) interface grows over several layers simultaneously. Figure 2 shows  $x$ - $y$  plots over the same time subinterval during the growth of four neighboring layers. The region in the top left corner of the computational box shows particles vibrating on lattice sites over four layers while the lower right indicates substantial disorder in those same layers. This behavior is also observed at "equilibrium" and is symptomatic of a rough interface. Irregular hill-and-valley structures at the interface form and reform dynamically as the system fluctuates around equilibrium. A similar trajectory analysis for the equilibrium (111) interface shows a transition from crystal to a highly mobile region to occur over one layer. Such a smooth interface is in keeping with the experimental observation that Si(111) is above its roughening temperature  $T_r$  and the spatial width of the transition region is similar to that observed in Lennard-Jones (100) and (111) molecular-dynamics simulations.<sup>15</sup> We cannot determine from our small finite-size systems whether these interfaces exhibit roughening behavior, but what is striking is the very dissimilar behavior of Si(100).  $T_r$  for Si(100) is so low that at the melting temperature the length scale for roughening fluctuations is apparently shorter than the dimensions of the computational cell. To our knowledge, this is the first three-dimensional molecular-dynamics simulation of crys-

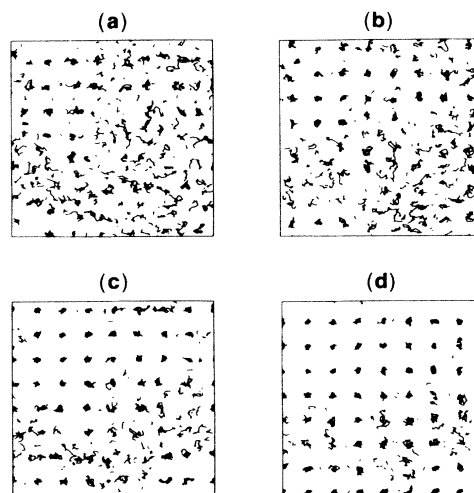


FIG. 2. Trajectory plots in  $x$ - $y$  plane of adjacent layers covering elapsed time between  $45\,000 \Delta t$  and  $50\,000 \Delta t$ . The depth range equals (a) 10.30–10.95, (b) 10.95–11.60, (c) 11.60–12.25, and (d) 12.25–12.90.

tal-fluid systems to indicate interface fluctuations characteristic of roughening. By way of rationalization of this behavior, we note that the nearest-neighbor bond model for Si predicts  $T_r=0$  for the (100) face because there is no in-plane fully connected bond network. Consequently, it costs zero energy to insert a step at the interface.<sup>16</sup>

Note the growth of a quasiliquid layer on the opposite side of the crystalline film during the (111) simulation. The quasiliquid layer remains after the system equilibrates. The shock wave, generated by the heat pulse, is able to overcome the nucleation barrier to quasiliquid-layer formation. The barrier is apparently more significant than that for the Lennard-Jones (111) or (100) faces since these surfaces melt both rapidly and with facility.<sup>14</sup> We discuss this point more fully elsewhere.<sup>17</sup> A similar mobile surface region is created at the Si(100) surface after the heat pulse but is less evident perhaps because the pulse was of lower magnitude (see earlier discussion). The evidence for a high-temperature quasiliquid layer on Si(111) is an attractive explanation for the  $1 \times 1$  LEED structures and the amorphous overlayer suggested by ion scattering. A further temperature-dependent study of the Si(111) crystal-vapor interface is required to pursue this point

further.

Figures 3 and 4 give the number-density  $\rho(z)$  and three-body energy-density  $E_3(z)$  profiles through the equilibrated systems. The (111) interface is sharp, the transition occurring over  $\sim 3$  reduced units of distance (0.6 nm). The three-body profile shows a large positive contribution in the liquid, where the coordination is near 8 and well away from tetrahedrality, and a small contribution in the crystal caused by the finite mean-square displacement of atoms away from lattice sites. Again, the quasiliquid region on the right-hand end of the crystal is evident. The (100) interface, in contrast, is broader being approximately 4 reduced units wide (0.8 nm). The ripples on the three-body profile on traversing the crystal-liquid interface nicely demonstrate the occurrence of both ordered and disordered regions within the same interfacial layers. Trajectory plots indicate significant diffusion for all  $z$  values less than 13.5. Lastly, note that both the (111) and (100) systems have a shoulder in  $\rho(z)$  at the liquid-vapor interface. This indicates a partially ordered structure at the interface which is not observed at simple liquid-vapor Lennard-Jones interfaces,<sup>18</sup> and which will be discussed in detail in a future paper.<sup>17</sup>

Table I gives the triple-point properties of the two

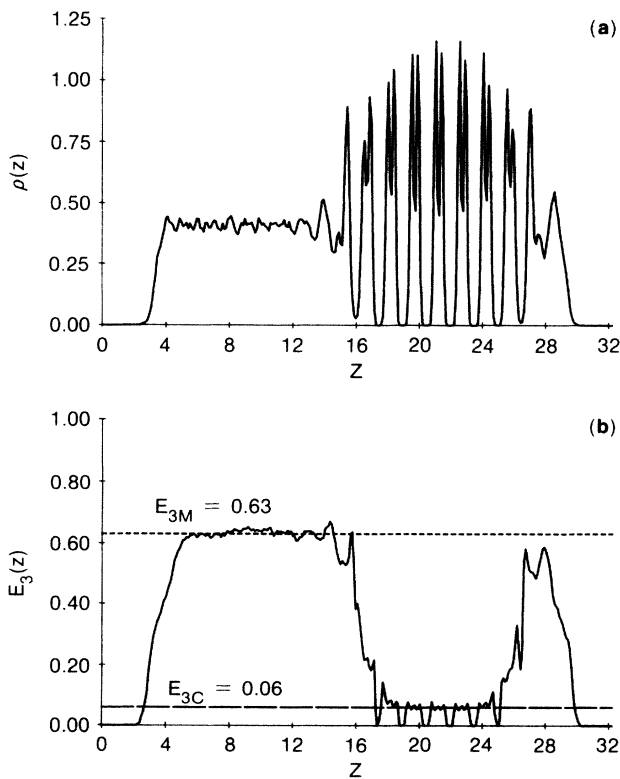


FIG. 3. (a) Equilibrium number density and (b) three-body potential energy density profiles for (111) triple-point system.

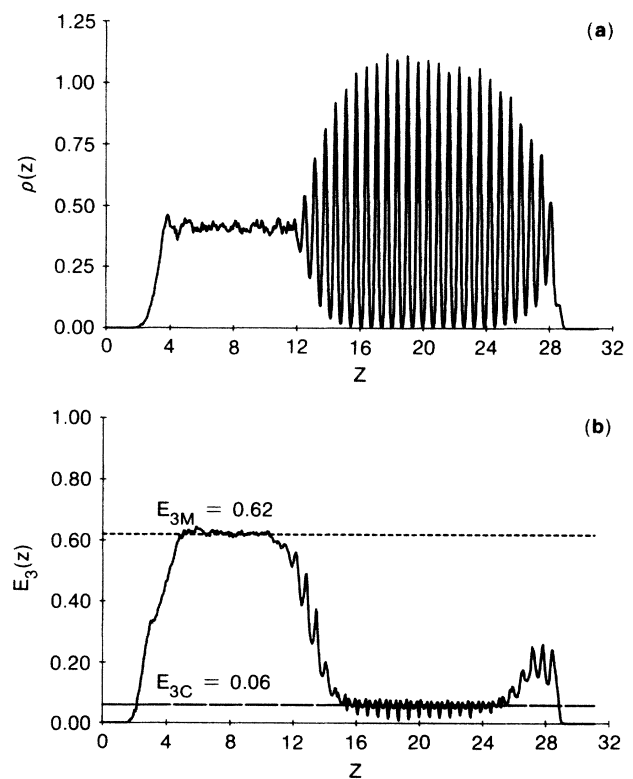


FIG. 4. (a) Equilibrium number density and (b) three-body potential energy density profiles for (100) triple-point system.

TABLE I. Triple-point properties in reduced units. Potential energies given per particle.

Surface	$T$	$E_C$	$E_M$	$E_{2C}$	$E_{2M}$	$E_{3C}$	$E_{3M}$	$L$	$\rho_C$	$\rho_M$
(111)	0.069(4)	-1.86	-1.72	-1.92	-2.35	0.06	0.63	0.14	0.45	0.49
(100)	0.070(2)	-1.86	-1.71	-1.92	-2.33	0.06	0.62	0.15	0.45	0.49

systems. They are in good agreement with one another. The melting point is  $\sim 1760$  K which is to be compared with the experimental value of 1683 K. The two-body energy of the liquid is actually lower than that of the crystal. This is consistent with the liquid having the higher coordination number. The three-body energy difference more than compensates for this, however, and a positive heat of fusion ( $L$ ) results. The calculated value of  $L$  of 30.3 kJ/mole<sup>19</sup> agrees poorly with an experimental value of 50.7 kJ/mole, and implies a sizable electronic contribution to the entropy of fusion. Notice that, in agreement with experiment, there is a density increase upon melting and the calculated values of 2.28 and 2.45 compare favorably with the experimental values of 2.30 and 2.53 g/cm<sup>3</sup>.<sup>20</sup> Lastly, the (essentially) zero concentration of particles in the vapor phase of the simulation is compatible with the low experimental triple-point pressure of  $\sim 10^{-1}$  Pa.<sup>21</sup> This latter quantity, assuming ideality, is equivalent to  $\sim 10^{-8}$  atom in the vapor volume of this simulation.

In conclusion, our simulations of silicon have shown for the first time the ability of the SW potential to describe satisfactorily a variety of triple-point properties and to explain growth characteristics which heretofore have been inferred from macroscopic experiment.

The work of one of us (J.Q.B.) was supported in part by an Olin Corporation Charitable Trust grant from the Research Corporation and by a contract from the U.S. Department of Energy (No. DE-FG02-85ER45218).

<sup>1</sup>P. N. Keating, Phys. Rev. **145**, 637 (1966).

<sup>2</sup>D. A. Smith, Phys. Rev. Lett. **42**, 729 (1979).

<sup>3</sup>F. H. Stillinger and T. A. Weber, Phys. Rev. B **31**, 5262 (1985).

<sup>4</sup>R. Biswas and D. R. Hamman, to be published.

<sup>5</sup>E. Pearson, T. Takai, T. Halicioglu, and W. A. Tiller, J. Cryst. Growth **70**, 33 (1984).

<sup>6</sup>B. W. Dodson and P. A. Taylor, Conference Abstracts, Materials Research Society Meeting, Boston, 1985 (unpublished).

<sup>7</sup>P. M. Petroff and R. J. Wilson, Phys. Rev. Lett. **51**, 199 (1983), and references therein.

<sup>8</sup>W. S. Yang and F. Jona, Phys. Rev. B **28**, 1178 (1983), and references therein.

<sup>9</sup>D. J. Chadi, J. Vac. Sci. Technol. **16**, 1290 (1979).

<sup>10</sup>M. T. Yin and M. L. Cohen, Phys. Rev. B **24**, 2303 (1981).

<sup>11</sup>F. F. Abraham and I. P. Batra, Surf. Sci. (to be published).

<sup>12</sup>T. Weber, private communication.

<sup>13</sup>T. F. Ciszek, J. Cryst. Growth **10**, 263 (1971).

<sup>14</sup>J. Q. Broughton and G. H. Gilmer, Acta Metall. **31**, 845 (1983).

<sup>15</sup>J. Q. Broughton, A. Bonissent, and F. F. Abraham, J. Chem. Phys. **74**, 4029 (1981).

<sup>16</sup>G. H. Gilmer, Mater. Sci. Enger. **65**, 15 (1984).

<sup>17</sup>F. F. Abraham and J. Q. Broughton, to be published.

<sup>18</sup>F. F. Abraham, in *Surface Science: Recent Progress and Perspectives*, edited by R. Vanselow (CRC Press, Cleveland, 1980).

<sup>19</sup>This value of  $L$  agrees favorably with the constant-density value extracted from Fig. 3 of SW's paper. The value quoted in their text is in error. F. H. Stillinger, private communication.

<sup>20</sup>V. M. Glazov, S. N. Chizhevskaya, and N. N. Glagoleva, *Liquid Semiconductors* (Plenum, New York, 1969).

<sup>21</sup>F. Rosebury, *Handbook of Electron Tube and Vacuum Techniques* (Addison-Wesley, Reading, Mass., 1965).